Journal of Korea Multimedia Society Vol. 20, No. 2, February 2017(pp. 205-215)
https://doi.org/10.9717/kmms.2017.20.2.205

Hippocampus Segmentation and Classification in Alzheimer's Disease and Mild Cognitive Impairment Applied on MR Images

Nuwan Madusanka[†], Yu Yong Choi[††], Kyu Yeong Choi[†††], Kun Ho Lee[††††], Heung-Kook Choi[†††††]

ABSTRACT

The brain magnetic resonance images (MRI) is an important imaging biomarker in Alzheimer's disease (AD) as the cerebral atrophy has been shown to strongly associate with cognitive symptoms. The decrease of volume estimates in different structures of the medial temporal lobe related to memory correlates with the decline of cognitive functions in neurodegenerative diseases. During the past decades several methods have been developed for quantifying the disease related atrophy of hippocampus from MRI. Special effort has been dedicated to separate AD and mild cognitive impairment (MCI) related modifications from normal aging for the purpose of early detection and prediction. We trained a multi-class support vector machine (SVM) with probabilistic outputs on a sample (n = 58) of 20 normal controls (NC), 19 individuals with MCI, and 19 individuals with AD. The model was then applied to the cross-validation of same data set which no labels were known and the predictions. This study presents data on the association between MRI quantitative parameters of hippocampus and its quantitative structural changes examination use on the classification of the diseases.

Key words: Alzheimer's Disease, Entropy, Cognitive Symptoms, Neurodegenerative Diseases, Classification

1. INTRODUCTION

Diagnosis of dementia is a trivial task in clinical routine. In brain imaging, clinical assessments by providing information about structural and functional, can be used for assisting the diagnosis using automated machine learning methods. Alzheimer's disease (AD) is the most common root of dementia, accounting for 60 - 80% of cases [1, 2]. Effective pre-symptomatic diagnosis and treatment of AD

※ Corresponding Author : Heung-Kook Choi, Address: Department of Computer Engineering, Inje University Injero 197, u-AHRC, Gimhae, Gyeongnam, 50834, Republic of Korea, TEL : +82-55-320-3437, FAX : +82-55-322-3107, E-mail : cschk@inje.ac.kr
Receipt date : Dec. 28, 2016, Approval date : Jan. 31, 2017
[†] Department of Computer Engineering, Inje University, Injero 197, u-AHRC, Gimhae, Gyeongnam, 50834, Republic of Korea
(E-mail : nuwanmadusanka@hotmail.com)
[††] National Research Center for Dementia, Chosun University, Pilmun-daero 309, Dong-gu, Gwangju, 61452, Republic of Korea
(E-mail : yuyongchoi@chosun.ac.kr)
[†††] National Research Center for Dementia, Chosun University, Pilmun-daero 309, Dong-gu, Gwangju, 61452, Republic of Korea
(E-mail : khaser@chosun.ac.kr)
[††††] National Research Center for Dementia, Chosun University, Pilmun-daero 309, Dong-gu, Gwangju, 61452, Republic of Korea
(E-mail : leekho@chosun.ac.kr)
[†††††] Department of Computer Engineering, Inje University, Injero 197, u-AHRC, Gimhae, Gyeongnam, 50834, Republic of Korea
※ This research was supported by Basic Science Research Program through the National Research Foundation of Korea(NRF) funded by the Ministry of Education (2015-059319). This research was also supported by the Brain Research Program through the National Research Foundation of Korea funded by the Ministry of Science, ICT & Future Planning (NRF-2014 M3C7A1046041).

could have vast public health benefits. The underlying pathology of AD precedes the onset of cognitive symptoms by many years, and efforts are underway to find reliable preclinical diagnostic biomarkers. The hippocampus is a vital temporal lobe structure in memory [3] and damage could be cause to multiple brain disorders including AD, depression, schizophrenia, traumatic brain injury, posttraumatic stress disorder, and mesial temporal sclerosis from temporal lobe epilepsy [4, 5]. In AD research, commonly-used structural MRI measures include whole-brain, entorhinal cortex [6], hippocampus, and temporal lobe volumes [7, 8], as well as ventricular enlargement. Reductions in hippocampus and entorhinal cortex volumes become apparent in the early stages of memory decline and may anticipate progression to MCI and AD [9]. Hippocampus atrophy measures from structural MRI are widely used; usually morphological features can detect more subtle alterations in the hippocampus that may provide even more sensitive detection of early changes in hippocampus.

The objective of this paper is to classify the AD, MCI and Normal Control (NC) group based on the hippocampus morphological features using machine learning techniques. The rest of the paper is organized as follows: Section 2 presents the material and methods. Section 3 presents the classification algorithms adopted and Section 4 describes experiments and results. Discussion of the work has been given in Section 5.

2. MATERIAL AND METHODS

2.1 MRI Data Acquisitions

Participants were recruited from a larger cohort of living subjects enrolled in the Chosun National University, National Dementia research center to Investigate dementia study within the Republic of Korea. All enrolled subjects undergo a clinical and informant-based interview, a comprehensive cognitive assessment including, physical examination, MRI brain scan and blood-screening tests as part of the scheduled protocol for diagnostic purposes. Potential participants for the current prospective study were randomly selected from the participant database according to clinical diagnosis. General inclusion criteria applicable to all subjects for this sub-study, were 60 years of age or older. The MR images used in this paper are obtained from the The Chosun National University, National dementia research center. The MRI scans are acquired using 1.5 Tesla, T1-weighted by Siemens scanner with TE/TI/TR = 2.98/900/2300 ms, slice thickness = 0.8 mm, Rows × Cols × Slices = 320 × 320 × 240, and voxel size of 0.8 × 0.8 × 0.8 mm^3. We acquired 58 subjects from The Chosun National University, National dementia research center database. Table 1 shows the characteristics of subjects used in this study.

Table 1. The Characteristics of subjects

	AD	MCI	NC
Numbers	71.3 ± 2.9	69.5 ± 3	69.5 ± 3
Age	71.3 ± 2.9	69.5 ± 3	69.5 ± 3
Sex (f/m)	10/9	10/9	10/10

Note: All data present in mean ± standard deviation mode. AD = Alzheimer's Disease patients, MCI = Mild Cognitive Impairment, NC = Normal Control patients.

2.2 Hippocampus Segmentation

A detailed description of the manual segmentation protocol of hippocampus is presented in this section. Manual tracing in a sample subject is illustrated for eight representative sagittal slices of the hippocampus in Fig. 1. Manual tracing of the hippocampus was performed by two expert rater with experience performing over 100 hippocampal tracings. Inter-rater reliability for first and a second expert rater, were measured for hippocampal volume and surface area measurements in a separate dataset using the intraclass correlation coefficient (ICC). Hippocampal volumes measured by first and second rater had inter-rater ICCs of 0.84

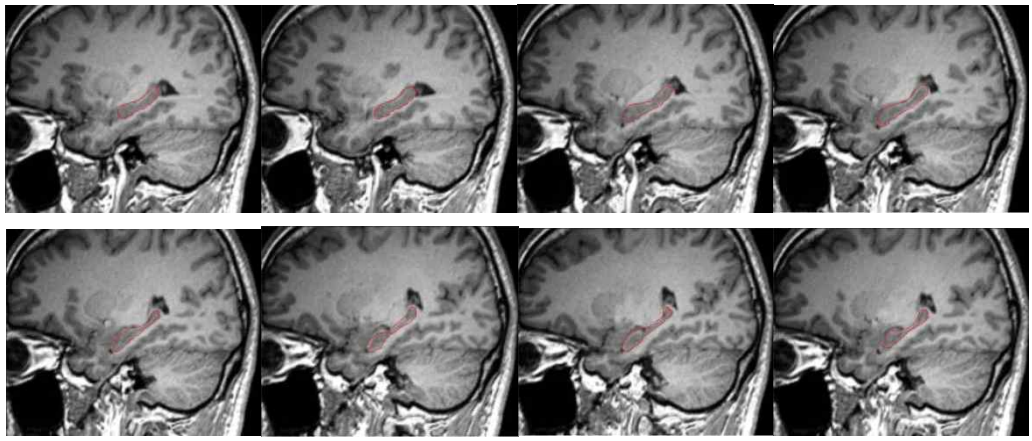

Fig. 1. A selection of manually segmented hippocampal sagittal slices of a representative subject.

for the left side and 0.86 for the right side. The ICCs ranged from 0.76 to 0.92 for inter-rater reliability of hippocampal volume readings. These indicate excellent agreement between and within these two observers. Manual tracing of the hippocampus was performed using a custom-built software system in native space and orientation on contiguous sagittal slices proceeding from the most posterior to most anterior slice.

2.3 Method

The proposed method for hippocampus segmentation and classification in AD and MCI patients from NC is shown in Fig. 2. Briefly, All MRIs were manually segmented. The Continuous Medial Representation framework (cm-rep) was used to extract the length of hippocampal medial axis and average thickness. Voxel based custom software (MRI-3DView) was used to calculated the hippocampal volume and surface area. In addition, the MSVMPack used as a classification framework.

2.3 Continuous Medial Representation Model

The medial representation (cm-rep) is a framework for shape analysis and shape-based normalization. Essentially a cm-rep model is a 3D geometrical model that defines the skeleton and the boundary of an object at the same time. The term skeleton is synonymous to the medial axis, although medial axes usually are described for 2D objects and we are dealing with 3D objects. In 3D, the medial axis (skeleton) is a surface or a set of

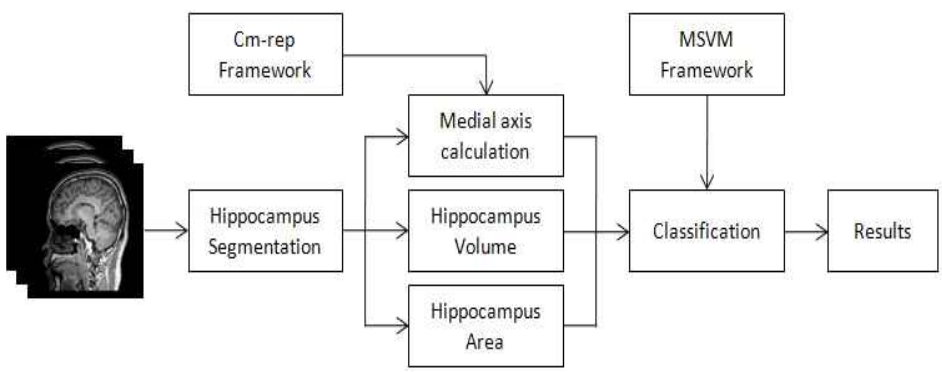

Fig. 2. The pipeline of proposed method for AD, MCI and NC classification based on hippocampus features.

surfaces. cm-rep models are deformable. During deformation, the correct geometric relationship between the boundary and the skeleton is maintained. The skeleton of a deformed model is still the correct geometrical skeleton of the boundary of the deformed model [10]. Also, during deformation, the topology of the skeleton (number of surfaces in the skeleton) does not change. The concept extends to 3D, where the medial axis is formed by a set of surfaces called medial manifolds in Fig. 3a. The medial axis is formed by uniformly thinning the object until a curve, or a set of curves, remains, as shown in Fig. 3b. The distance from the medial axis to the boundary is an easily inferred morphological feature describing thickness.

The cm-rep approach models shape by defining a synthetic skeleton, consisting of a medial manifold $\Omega \rightarrow \mathbb{R}^3$ and a radial $\Omega \rightarrow \mathbb{R}^+$, both continuous parametric functions defined on a domain $\Omega \rightarrow \mathbb{R}^2$. The boundary is derived from the synthetic skeleton using inverse skeletonization [11]. Inverse skeletonization shown by following form:

$$b^{\pm} = m + R\vec{U}^{\pm},\ where\ \vec{U}^{\pm} = -\nabla_m R \pm \sqrt{1 - \|\nabla_m R\|^2}\,\overrightarrow{N_m} \quad (1)$$

The boundary b is formed by two halves b^+ and b^- that are located on opposite sides of the medial manifold. Vectors $\vec{U}^+$ and $\vec{U}^-$ point from the medial manifold to the boundary, have unit length, and are orthogonal to the boundary. They are defined in terms of ∇_mR, the Riemannian gradient of R on m, and $\overrightarrow{N_m}$, the unit normal to m. The vector ∇_m is the gradient of the thickness scalar field on the medial surface. The concept of inverse skeletonization is illustrated in Fig. 1c-d.

$$\nabla_m = [m_u \ \ m_v]\, I_m^{-1} \begin{bmatrix} r_u \\ r_v \end{bmatrix} \quad (2)$$

where I_m is the metric tensor on the medial surface.

The projections of both boundary counterparts onto the medial tangent plane lie in the negative ∇_m direction. The distance from each counterpart to the medial tangent plane is $\sqrt{1 - \|\nabla_m\|^2}$; hence the boundary counterparts of m are defined only if .

2.3 Hippocampus Volume and Surface Area Calculation

Hippocampal volume and surface area is a marker sensitive to disease state and progression in Alzheimer's disease (AD). In this study we have calculated hippocampus volume and surface area of each participant as most significant features which are associated with AD and MCI patients. This facts have been proved by previous studies related to . Hippocampus volumetry calculated by multiplying the voxel size with total number of voxels that are presented in hippocampus. Surface area oh the hippocampus calculated by multiplying the pixel size with total number of surface pixels

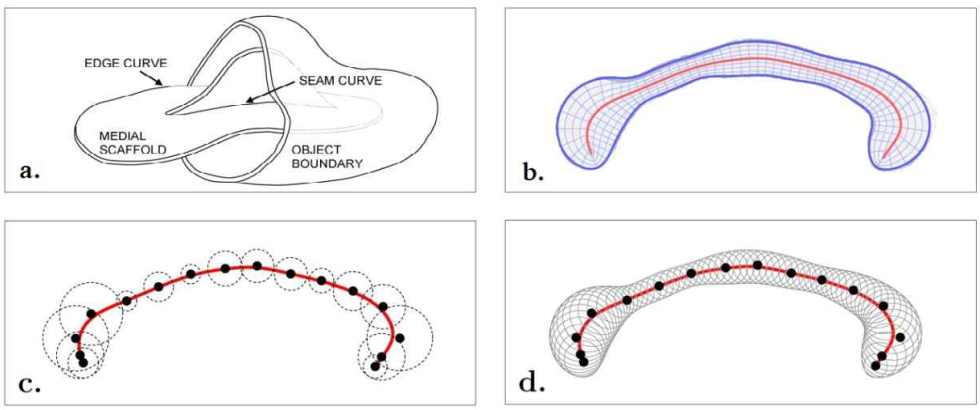

Fig. 3. An illustration of medial geometry and the cm-rep method with 2D and 3D examples.

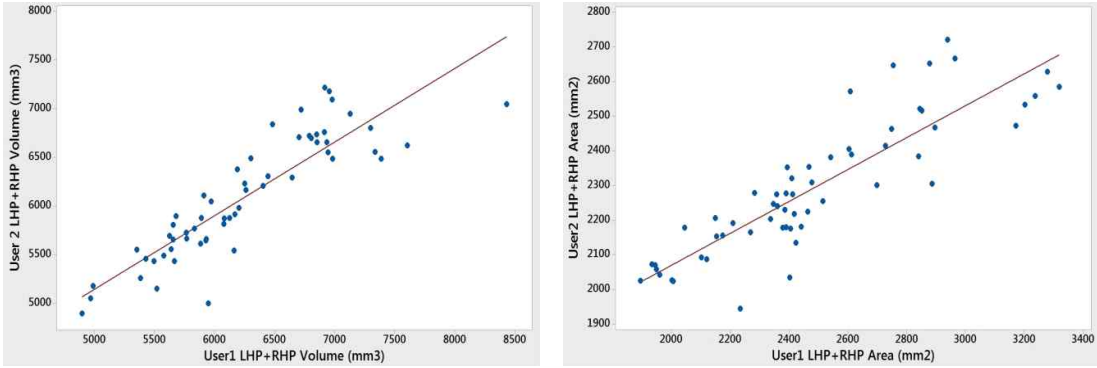

Fig. 4. Manual segmented hippocampus volume and surface on 1.5T scans, There is good correlated between two expert users.

in the hippocampus.

Inter-rater reliability for two expert rater, were measured for hippocampus volume and surface area measurement using R-square value. R-square value for hippocampus volume and area were 77.40 % and 75.88% respectively as shown in Fig. 4.

3. CLASSIFICATION

The classification features were selected based on the morphological changes of hippocampus between AD, MCI and NC patients. Specifically, each subject was represented as two sets (left/right hippocampus) of three-dimensional object [12]. When considering the features extraction we were selected significant features which are directly related with AD, each subject can thus be represented by a feature vector of size 58. The Multi-Class Support Vector Machine (MSVM) algorithm used to classify the data.

3.1 Support Vector Machine (SVM)

Support Vector Machine is essentially a two classification method, but in many practical applications for multi-class classification problem, how to promote the excellent performance of support vector machine to multiclass classification has become a hot issue in the study. Support vector machine is a very specific class of algorithms, characterized by the use of kernels, the absence of local minima, the sparseness of the solution and the capacity control obtained by acting on the margin, or on other 'dimension independent' quantities such as the number of support vectors[13-15].

3.2 Linear SVM Classifiers

Let us begin with the simplest case, in which the training patterns are linearly separable. That is, there exists a linear function of the form

$$f(x) = w^T x + b \quad (3)$$

such that for each training example $f(x_i) \geq 0$ for $y_i = +1$, and $f(x_i) < 0$ for $y_i = -1$. In other words, training examples from the two different classes are separated by the hyperplane $f(x) = w^T x + b = 0$.

For a given training set, while there may exist many hyperplanes that separate the two classes, the SVM classifier is based on the hyperplane that maximizes the separating margin between the two classes. In other words, SVM finds the hyperplane that causes the largest separation between the decision function values for the "borderline" examples from the two classes. Mathematically, this hyperplane can be found by minimizing the following cost function:

$$J(w) = \frac{1}{2} w^T w = \frac{1}{2} \|w\|^2 \quad (4)$$

subject to the separability constraints

$$w^T x_i + b \geq +1, \quad for\ y_i = +1$$

or

$$w^T x_i + b \leq -1, \quad for\ y_i = -1;\ i = 1,2,\ldots..,l \quad (5)$$

Equivalently, these constraints can be written more compactly as

$$y_i(w^T x_i) \geq 1;\ \ i = 1,2,\ldots..,l \quad (6)$$

This specific problem formulation may not be useful in practice because the training data may not be completely separable by a hyperplane. In this case, slack variables, denoted by ξ_i, can be introduced to relax the separability constraints in (6) as follows:

$$y_i(w^T x_i + b) \geq 1 - \xi_i\ ,\ \xi_i \geq 0;\ \ i = 1,2,\ldots..,l \quad (7)$$

Accordingly, the cost function in (4) can be modified as follows:

$$J(w,\xi) = \frac{1}{2}\|w\|^2 + C\sum_{i=0}^{l}\xi_i \quad (8)$$

where is a user-specified, positive, regularization parameter. In (8), the variable is a vector containing all the slack variables $\xi_i = 1,2,\ \ldots\ \ l$.

The modified cost function in (8) constitutes the so-called *structural risk*, which balances the *empirical risk* (i.e., the training errors reflected by the second term) with model complexity (the first term). The regularization parameter controls this trade-off. The purpose of using model complexity to constrain the optimization of empirical risk is to avoid overfitting, a situation in which the decision boundary too precisely corresponds to the training data, and thereby fails to perform well on data outside the training set.

3.3 Nonlinear SVM Classifiers

The linear SVM can be readily extended to a nonlinear classifier by first using a nonlinear operator Φ(.) to map the input pattern x into a higher dimensional space H. The nonlinear SVM classifier so obtained is defined as

$$f(x) = w^T\Phi(x) + b \quad (9)$$

which is linear in terms of the transformed data, but nonlinear in terms of the original data $x\epsilon R^n$. Following nonlinear transformation, the parameters of the decision function are determined by the following minimization:

$$\min j(w,\xi) = \frac{1}{2}\|w\|^2 + C\sum_{i=0}^{l}\xi_i \quad (10)$$

subject to

$$y_i(w^T\Phi(x_i) + b) \geq 1 - \xi_i, \xi_i \geq 0; i = 1,2,\ldots..,l \quad (11)$$

3.4 Multi-Class Support Vector Machine (MSVM)

Multi-class linear classification in the one-versus-one setting is not well suited for classification of NC, MCI, and AD, because MCI is in between NC and AD. We therefore employed a non-linear SVM with radial basis function. For classification, we used one versus all support vector machine (SVM) package named MSVMPack with the option for probabilistic multi-class outputs [17].

The MSVMPack is an open source package dedicated to multi-class support vector machines, SVMs which can handle classification problems with more than two classes without relying on decomposition methods. The aim is to provide a unified framework and implementation for all the different MSVM models in a single package [18].

The default behavior of training function is to keep training until a predefined level of accuracy is reached in terms of the ratio, thus defining the stopping criterion as R > 1 - ε. The value of the accuracy level 1 - ε can be set through the option -a.

$$R = \frac{Value\ of\ the\ dual\ objective\ function}{upper\ bound\ on\ the\ optimum} \quad (12)$$

MSVMPack implements k-fold cross validation by first computing a random permutation of the data instances and then dividing the data set in k subsets of equal size. This random permutation is made to easy the obtaining of subsets that contain examples of all categories in the typical case where the data set is sorted with respect to the class labels.

Table 2. The group comparison of hippocampus features between users

	User1			User2		
	AD	MCI	NC	AD	MCI	NC
Hippocampus Volume (mm^3)	6212.61 ±71.68	6825.21 ±169.79	6877.66 ±391.00	5852.41 ±439.87	6573.57 ±114.40	6627.84 ±110.06
Hippocampus Area (mm^2)	2452.80 ±89.15	2491.84 ±159.74	2808.32 ±112.23	2266.56 ±15.84	2292.16 ±143.38	2359.36 ±77.38
Hippocampus Medial axis (mm)	40.78 ±1.84	40.92 ±2.41	41.38 ±2.17	39.46 ±1.42	40.04 ±0.92	41.56 ±1.27
Hippocampus Thickness (mm)	8.45 ±0.68	8.72 ±1.32	9.16 ±1.04	8.26 ±1.06	8.66 ±1.46	8.93 ±1.28

4. RESULTS

4.1 Hippocampus Segmentation Results

In total 58 subjects are belong to three classes (AD, MCI and NC), two experts were manually delineated and segment the hippocampus. The right and left hippocampus volumes are calculated and accumulated. Fig. 2 shows the association between two expert users' segmented hippocampus volumes and surface in the AD, MCI and NC participants. In addition, Table 2 shows the all features which are calculated from the segmented hippocampus for all groups.

According to Table 2, it is clear that AD participants show smaller hippocampus volume, surface area, medial axis and thickness in both users' results, because of small number participants in this research, we didn't conduct any age and gender-matched comparison between AD,MCI and NC groups. Comparing the results of statistical mean between patients with AD and normal control group, there are significant differences of feature values in both cases. In addition, when comparing the results of statistical mean between patients with MCI and normal control group, there aren't significant differences in both cases.

The classification process is fully automatic. Using a single core (Intel Core i5, 3.40Ghz) per subject the total computational time was approximately 15 minutes distributed on training (15 min), and applying the classifier after it has been trained takes only a few seconds. The classification results were obtained for the training set (n = 58) by cross-validation, and on the validation set (n = 20) by applying the Gaussian Radial Basis Function (RBF) the model trained on the entire training set. Test accuracy of classification of the validation (training) set of recognition accuracy was 65.43% and 67.26% respectively for user 1 and user 2.

According to Table 3, it is clear that AD patients and NC group classification accuracy is higher compare with MCI patients. In addition to this, when MCI patient and NC classification accuracy has too lower value. This clearly demonstrate, that MCI and NC have very similar feature values and has confusion in identification.

Table 3. Confusion matrix of classification of AD,MCI and NC groups based on different users

User 1				
Test / Actual	AD	MCI	NC	Accuracy (%)
AD	15	3	1	78.94
MCI	5	7	7	36.84
NC	1	4	15	75.00
User 2				
AD	16	3	0	84.42
MCI	3	9	7	47.36
NC	2	4	14	70.00

5. DISCUSSION

In this research, we attempted to classify Alzheimer disease, Mild Cognitive Impairment and normal control group based on hippocampus morphological features using machine learning algorithms. It has also proven its usefulness in discriminating between cognitively normal subjects, patients with MCI or AD in a setting which corresponds better to clinical routine. In our method, we used manual hippocampus segmentation approaches; because of hippocampus manual segmentation accuracy outperform than any existing semi-automatic and fully automatic segmentation algorithms. In morphological features calculation segmentation accuracy directly affect on the morphological feature values. In segmentation process, to minimize the human error, we used two expert users to segment all datasets without labels and calculate the inter-rater reliability. Hippocampus morphological features extraction and classification done by cm-rep framework and multi-class support vector machine (MSVM) to examine the volume and shape changes in hippocampus with AD and MCI disease compare with the normal control group. In more detail, cm-rep shape analysis demonstrated greater global shape changes in the hippocampus. In this study, we focused on several specific features including hippocampus volumes in patients with AD and MCI compared to cognitively normal subjects. The results show consistently significant findings from accuracy, sensitivity and specificity measures in contrast to earlier research. The results of this study revealed that the reduction and shape changes in hippocampus region have strong relationship with AD, while MCI shows lower classification accuracy with both AD and NC groups. Our classification results prove that there is a link between hippocampus morphological changes in AD.

REFERENCE

[1] C.P. Hughes, L. Berg, W.L. Danziger, L.A. Coben, and R.L. Martin, "A New Clinical Scale for the Staging of Dementia," *The British Journal of Psychiatry*, Vol. 140, pp. 566-572, 1982.

[2] M. Folstein, S.E. Folstein, and P.R. McHugh, "Mini-mental State: A Practical Method for Grading the Cognitive State of Patients for the Clinician," *Journal of Psychiatric Research*, Vol. 12, No. 3, pp. 189-198, 1975.

[3] J.M. Schott, S.L. Price, C. Frost, J.L. Whitwell, M.N. Rossor, and N.C. Fox, "Measuring Atrophy in Alzheimer Diseases: A Serial MRI Study over 6 and 12 Months," *Neurology*, Vol. 65, No. 1, pp. 119-124, 2005.

[4] J.C. Pruessner, D.L. Collins, M. Pruessner, and A.C. Evans, "Age and Gender Predict Volume Decline in the Anterior and Posterior Hippocampus," *Journal of Neuroscience*, Vol. 21, No. 1, pp. 194-200, 2001.

[5] T. Selma, N. Madusanka, T.H. Kim, Y.H. Kim, C.W. Mun, and H.K. Choi, "Contrast-enhanced Bias-corrected Distance-regularized Level Set Method Applied to Hippocampus Segmentation," *Journal of Korea Multimedia Society*, Vol. 19, No. 8, pp. 1236-1247, 2016.

[6] C.R. Jack, M.M. Shiung, J.L. Gunter, P.C. O'Brien, S.D. Weigand, D.S. Knopman, et al, "Comparison of Different MRI Brain Atrophy Rate Measures with Clinical Disease Progression in AD," *Neurology*, Vol. 62, No. 4, pp. 591-600, 2004.

[7] J. Yang, L.H. Staib, and J.S. Duncan, "Neighbor-constrained Segmentation with Level Set Based 3D Deformable Models," *IEEE Transactions on Medical Imaging*, Vol. 23, No. 8, pp. 940-948, 2004.

[8] Y.S. Izmantoko, H.S. Yoon, E. Adiya, C.W. Mun, Y. Huh, and H.K. Choi, "Implementation of 2D Active Shape Model-based Segmentation on

Hippocampus," *Journal of Korea Multimedia Society*, Vol. 17, No. 1, pp. 1-7, 2014.

[9] M. Benjelloun, S. Mahmoudi, and F. Lecron, "A Framework of Vertebral Segmentation Using the Active Shape Model-based Approach," *International Journal of Biomedical Imaging*, Vol. 2011, pp. 1-14, 2011.

[10] P.A. Yushkevich, J.A. Detre, D.M. Hamilton, M.A.F. Seara, K.Z. Tang, A. Hoang, et al, "Hippocampus-Specific fMRI Group Activation Analysis Using the Continuous Medial Representation," *NeuroImage*, Vol. 35, No. 4, pp. 1516-1530, 2007.

[11] S. Bouix, J.C. Pruessner, D.L. Collins, and K.Siddiqi, "Hippocampal Shape Analysis Using Medial Surfaces," *NeuroImage*, Vol. 25, No. 4, pp. 1077-1089, 2005.

[12] J.C. Mazziotta, A. Toga, A. Evans, P. Fox, J. Lancaster, K. Zilles, et al, "A Probabilistic Atlas and Reference System for the Human Brain: International Consortium for Brain Mapping (ICBM)," *Philosophical Transactions of the Royal Society of London*, Vol. 356, No. 1412, pp. 1293-1322, 2001.

[13] K.H. Fritzsche, A. Von Wangenheim, D.D. Abdala, and H.P. Meinzer, "A Computational Method for the Estimation of Atrophic Changes in Alzheimer's Disease and Mild Cognitive Impairment," *Computerized Medical Imaging and Graphics*, Vol. 32, No. 4, pp. 294-303, 2008.

[14] J. Wang, A. Ekin, and G. deHaan, "Shape Analysis of Brain Ventricles for Improved Classification of Alzheimer's Patients," *Proceeding of International Conference Image Processing*, pp. 2252-2255, 2008.

[15] C. Cortes and V. Vapnik, "Support-Vector Networks," *Machine Learning*, Vol. 20, pp. 273-297, 1995.

[16] J. Czajkowska, M. Rudzki, and Z. Czajkowski, "A New Fuzzy Support Vectors Machine for Biomedical Classification," *Proceeding of 30th Annual International IEEE EMBS Conference*, pp. 4476-4479, 2008.

[17] F. Bovolo, L. Bruzzone, and L. Carlin, "A Novel Technique for Subpixel Image Classification Based on Support Vector Machine," *IEEE Transaction on Image Processing*, Vol. 19, No. 11, pp. 2983-2999, 2010.

[18] V. Vapnik, "An Overview of Statistical Learning Theory," *IEEE Transactions on Neural Networks*, Vol. 10, No. 5, pp. 988-999, 1999.

Nuwan Madusanka

He received the B.S. degree in Computer Science from Uva Wellassa University, Sri Lanka in 2011, the M.S. degree in School of Computer Engineering from Inje University, Gimhae, Korea in 2015. He is currently a Ph.D. student in Medical Image Technology Laboratory (MITL), School of Computer Engineering, Inje University, Korea. From 2011 to 2013, he worked as a software engineer for reputed software company in Sri Lanka, where he involved the projects in smart phone based application development. From 2013 to present, he is working as a research student for Medical Image Technology Laboratory. His current research interests include image processing, image analysis and visualization.

Yu Yong Choi

He received the B.S. degree in computer engineering from Seoul National University, Seoul, Korea in 1993, the M.S. degree in computer engineering from Seoul National University, Seoul, Korea in 1995, and the Ph.D. degree in interdisciplinary program in neuroscience from Seoul National University, Seoul, Korea in 2008. From 2006 to 2009, he worked as a researcher for Laxtha Research and Development Institute, where he developed a technique to measure human intelligence using brain images. From 2009 to 2010, he worked as a researcher and lecturer for Research Institute for Image and Cultural Content in Dongguk University where he studied cognitive enhancement techniques through computer games. From 2010 to 2013, he worked as a research professor for Hanyang University and Gwangju Institute of Science and Technology. In 2014, he joined Chosun University, Gwangju, Korea, and currently works at the National Research Center for Dementia (NRCD) as a co-investigator. His current research interests include early detection of dementia onset and cognitive enhancement.

Kyu Yeong Choi

He received the B.S. degree in Electrical engineering from Korea Advanced Institute of Science and Technology, Daejon, Korea in 1995, the M.S. degree in Life Science from Gwangju Institute of Science and Technology (GIST), Gwangju, Korea in 1998, and the Ph.D. degree in Life Science from GIST, Gwangju, Korea in 2003. From 2003 to 2006, he worked as a Postdoctoral researcher at GIST, where he investigated the role of SPIN90, one of acting binding protein, in neuronal cell morphogenesis. From 2006 to 2012, he worked as a visiting/research fellow at National Institutes of Health, Bethesda, MD, US, where he investigated the stimulus-driven regulation of mGluR5 synaptic protein. From 2012 to 2014, he worked as a research professor at GIST, where he addressed the role of mGluR5 protein in synaptic plasticity. In 2014, he joined as a co-investigator at the National Research Center for Dementia (NRCD), Chosun University, Gwangju, Korea. His current research interests include early detection of dementia onset and the role of genetic variants on onset of AD.

Kun Ho Lee

He received the B.S. degree (1989) at Department of Genetic Engineering, Korea University, Seoul, Korea, the M.S. dgree (1992) and Ph.D. degree (1998) at Department of Molecular Biology, Seoul National University, Seoul, Korea. From 1998 to 1999, he worked as a Post-doctoral fellow at the Center for Cell Differentiation and then moved to Department of Pharmacology, School of medicine, University of Pittsburgh to extend his research as a Research Associate for one and half year. After comeback to Seoul, he focused on neuroimaging study at the Korea Institute of Brain Science for three years. From 2004 to 2009, he joined the Brain Research Center at Seoul National University, where he worked on the development of neurometric model of human intelligence based on MR imaging. In 2009, he moved to Chosun University, Gwangju, Korea, and work at the National Research Center for Dementia (NRCD) as the director and is also affiliated at College of Natural Sciences. His current research interests include brain image analysis and development of prediction model of neurodegenerative diseases based on MR imaging.

Heung-Kook Choi

He has gone undergraduate studying and graduate studying in Computer Science and Engineering at the Department of Electrical Engineering of Linköping University, Sweden (1984-1990) and Ph.D studying in computerized image analysis at the center for image Image Analysis of Uppsala University, Sweden (1990-1996). He was President of Industry and Academic Cooperation Foundation at Inje University. His interesting research fields are in computer graphics, virtual reality, medical image processing and analysis.